

# Sticky Monolayers and Defect-Free Langmuir–Blodgett Bilayers Using Poly(acrylamide) Glue

Junwei Li, Vaclav Janout, and Steven L. Regen\*

Department of Chemistry, Lehigh University, Bethlehem, Pennsylvania 18015

Received July 26, 2006. Revised Manuscript Received August 22, 2006

The introduction of poly(acrylamide) (PAM,  $M_w$  10 000) to an aqueous subphase resulted in increased intermolecular association in the monolayer formed from 5,11,17,23,29,35-hexaamideoxime-37,38,39,40,41,42-hexakis(1-hexadecyloxy) calix[6]arene (**2**) at the air–water interface, as evidenced by surface viscosity measurements. Langmuir–Blodgett (LB) bilayers of **2**, which were deposited onto silylated silicon wafers, showed the presence of PAM, as determined by X-ray photoelectron spectroscopy (XPS). On the basis of XPS analysis at two different takeoff angles (15 and 75°), both the amidoxime groups of the calix[6]arene and the amide groups of PAM, appear to be buried within the LB bilayer. Deposition of single LB bilayers of **2** containing PAM onto poly[1-(trimethylsilyl)-1-propyne] (PTMSP) supports and measurement of their permeability with respect to He, N<sub>2</sub>, and CO<sub>2</sub> showed a substantial improvement in their permeation selectivity properties, compared with analogous membranes that were devoid of PAM. Taken together, these results indicate that the use of nonionic, water-soluble polymers that are capable of hydrogen bonding with surfactant monolayers have considerable promise as “gluing” agents for enhancing the cohesiveness and quality of corresponding LB films.

## Introduction

Langmuir–Blodgett (LB) films have been investigated extensively over the past 70 years, with considerable attention being paid to their nonlinear optical, piezoelectric, pyroelectric, semiconducting, sensing, and barrier properties.<sup>1–5</sup> One significant problem that has limited the practical development of these materials has been their film quality. In particular, the fabrication of defect-free LB bilayers has proven to be a major challenge.<sup>6</sup>

Recently, we introduced the concept of “gluing”, whereby a water-soluble polyelectrolyte is used to ionically cross-link Langmuir–Blodgett (LB) monolayers of surfactants bearing multiple counterions.<sup>7</sup> We also showed that such gluing can eliminate film defects, as evidenced by changes in their barrier properties. For example, two monolayers of

calix[6]arene **1** that were glued with poly(styrene sulfonate) (PSS,  $M_w$  30 000–50 000) exhibited a He/N<sub>2</sub> gas permeation selectivity of ca. 250 (Chart 1).<sup>7a</sup> Given the extreme thinness of these membranes, such selectivity is exceptional.<sup>8</sup> In the absence of PSS, analogous LB films show no selectivity toward He and N<sub>2</sub>.

In the work that is reported herein, our primary aim was to expand the concept of glued LB bilayers beyond that of ionic cross-linking. Specifically, we have tested the feasibility of using hydrogen bonding and hydrophobic interactions between a nonionic, water-soluble polymer and a surfactant monolayer to enhance the cohesiveness of the monolayer and to allow for the construction of defect-free LB films.

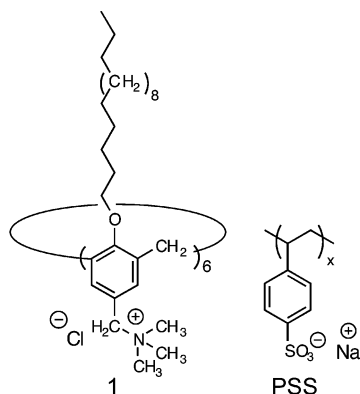
## Experimental Section

**Methods and Materials.** Unless stated otherwise, all reagents and chemicals were obtained from commercial sources and used

- \* To whom correspondence should be addressed. E-mail: sl0@lehigh.edu.
- (1) Blodgett, K. A. *J. Am. Chem. Soc.* **1935**, *57*, 1007–1022.
  - (2) Blodgett, K. A. *Film Structure and Method of Preparation*, U.S. Patent 2220860, 1940.
  - (3) Ulman, A. *An Introduction to Ultrathin Films: From Langmuir–Blodgett to Self-Assembly*; Academic Press: New York, 1991.
  - (4) Gaines, G. L., Jr. *Insoluble Monolayers at Liquid–Gas Interfaces*; Interscience: New York, 1966.
  - (5) Roberts, G. G. *Langmuir–Blodgett Films*; Plenum Press: New York, 1990.
  - (6) (a) Rose, G. D.; Quinn, J. A. *Science* **1968**, *159*, 636–637. (b) Albrecht, O.; Laschewsky, A.; Ringsdorf, H. *Macromolecules* **1984**, *17*, 937–940. (c) Higashi, N.; Kunitake, T.; Kajiyama, T. *Polym. J.* **1987**, *19*, 289–291. (d) Stroeve, P.; Coelho, M. A. N.; Dong, S.; Lam, P.; Coleman, L. B.; Fiske, T. G.; Ringsdorf, H.; Schneider, J. *Thin Solid Films* **1989**, *180*, 241–248. (e) Bruinsma, P.; Stroeve, P. *Thin Solid Films* **1994**, *244*, 958–961. (f) Tebbe, H.; Ackern, F. van; Tieke, B. *Macromol. Chem. Phys.* **1995**, *196*, 1475–1486. (g) Zhou, P.; Samuelson, L.; Alva, S.; Chen, C.-C.; Blumenstein, R. B.; Blumenstein, A. *Macromolecules* **1997**, *30*, 1577–1581. (h) Steehler, J. K.; Lu, W.; Kemery, P. J.; Bohn, P. W. *J. Membr. Sci.* **1998**, *139*, 243–257. (i) Marek, M.; Brynda, E.; Pientka, Z.; Brozova, L. *Macromol. Rapid Commun.* **1998**, *19*, 53–57.

- (7) (a) Yan, X.; Janout, V.; Hsu, J. T.; Regen, S. L.; *J. Am. Chem. Soc.* **2003**, *125*, 8094–8095. (b) Li, J.; Janout, V.; Regen, S. L. *Langmuir*, **2004**, *20*, 2048–2049. (c) Li, J.; Janout, V.; McCullough, D. H., III; Hsu, J. T.; Troung, Q.; Wilusz, E.; Regen, S. L. *Langmuir* **2004**, *20*, 8214–8219. (d) McCullough, D. H., III; Janout, V.; Li, J.; Hsu, J. T.; Troung, Q.; Wilusz, E.; Regen, S. L. *J. Am. Chem. Soc.* **2004**, *126*, 9916–9917. (e) Li, J.; Janout, V.; Regen, S. L. *Langmuir*, **2005**, *21*, 1676–1678. (f) McCullough, D. H., III; Regen, S. L. *Chem. Commun.* **2004**, 2787–2791. (g) Li, J.; Janout, V.; Regen, S. L. *J. Am. Chem. Soc.* **2006**, *128*, 682–683.
- (8) For a review of organic membranes and transport mechanisms for gas permeation, see: (a) Stern, S. A. *J. Membr. Sci.* **1994**, *94*, 1–65. (b) Koros, W. J.; Fleming, G. K. *J. Membr. Sci.* **1993**, *83*, 1–80. (c) Koros, W. J. *Chem. Eng. Prog.* **1995**, *91*, 68–81. (d) Robeson, L. M.; Burgoyne, W. F.; Langsam, M.; Savoca, A. C.; Tien, C. F. *Polymer* **1994**, *35*, 4970–4978. (e) *Polymers For Gas Separations*; Toshima, N., Ed.; VCH Publishers: New York, 1992. (f) Robeson, L. M. *J. Membr. Sci.* **1991**, *62*, 165–185. (g) Robeson, L. M. *J. Membr. Sci.* **1991**, *62*, 165–185. (h) Freeman, B. D. *Macromolecules*, **1999**, *32*, 375–380.

Chart 1



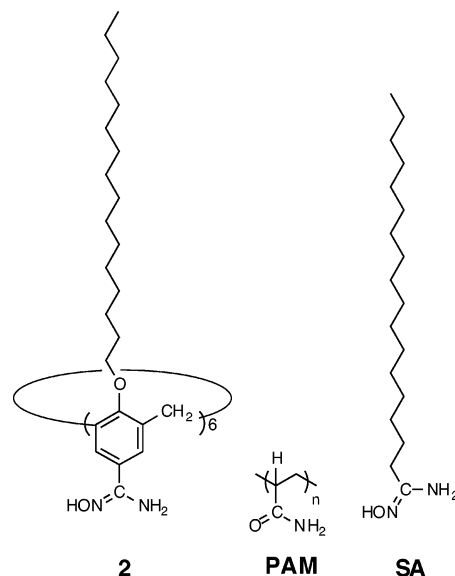
without further purification. House-deionized water was purified using a Millipore Milli-Q-filtering system containing one carbon and two ion-exchange stages. Chloroform/methanol (9/1,v/v) that was used as a spreading solvent was prepared from HPLC grade Burdick and Jackson solvents. Methods that were used to prepare 5,11,17,23,29,35-hexaamidoxime-37,38,39,40,41,42-hexakis(1-hexadecyloxy)calix[6]arene (**2**) were similar to those previously described.<sup>9</sup> Poly(acrylamide) ( $M_w$  10 000, Aldrich) was used as obtained. Poly[1-(trimethylsilyl)-1-propyne (PTMSP) ( $M_w = 8 \times 10^5$  (intrinsic viscosity), which was used as support material, was a gift from Air Products and Chemicals.

**Surface Pressure–Area Isotherms.** All monolayer measurements and LB film fabrications were made using a Nima 612D film balance (Nima Technologies, Coventry England), equipped with a LB dipper. All isotherms were determined at 25 °C. Surfactant solutions (1 mg/mL) were spread onto the aqueous subphase having a surface area of 600 cm<sup>2</sup>, using a gastight, 50  $\mu$ L Hamilton syringe. Exact concentrations were determined by direct weighing of aliquots after evaporation of solvent using a Cahn 27 electrobalance. In all cases, spreading solvents were allowed to evaporate for at least 30 min prior to compression under a flow of nitrogen.

**Surface Viscosity Measurements.** For surface viscosity experiments, a home-built canal viscometer (192 mm  $\times$  40 mm solid Teflon block, having a centrally located 6.0 mm slit) was placed in front of the compressing barrier and the monolayer was compressed at a rate of 25 cm<sup>2</sup>/min.<sup>9</sup> Compressions were stopped when a target pressure of 20 dyn/cm was reached. The resulting monolayer was then allowed to equilibrate at this pressure for 1 h. After this period of time, the moving barrier was expanded at the maximum speed of 120 cm<sup>2</sup>/min, leaving the canal viscometer at its original position. The resulting surface pressure was then recorded as a function of time. The rate of surface pressure decrease was taken as a measure of the surface viscosity of the monolayer.

**Fabrication of Composite Membranes and Gas Permeation Measurements.** PTMSP membranes (around 30  $\mu$ m thick) were used as supports for the fabrication of composite membrane. The casting technique of PTMSP membrane has been reported before.<sup>9</sup> PTMSP/surfactant composite membranes were prepared by conventional vertical Langmuir–Blodgett (LB) “dipping”. All transfers were performed in a positive pressure clean room. The dipping speed that was used for each monolayer transfer was 2 mm/min. Each composite membrane was allowed to remain in the laboratory ambient (clean room) for a minimum of 12 h before gas permeation measurements were carried out. Gas permeation measurements were made with a home-built stainless steel apparatus.<sup>9</sup>

Chart 2



**Substrate Preparation.** For ellipsometric and XPS measurements, the LB bilayer was transferred onto *n*-octadecyltrichlorosilane (OTS)-treated silicon substrates. The wafers (WaferNet, Inc., San Jose, CA) were cut into 15  $\times$  25 mm pieces and treated in concentrated H<sub>2</sub>SO<sub>4</sub> and 30% H<sub>2</sub>O<sub>2</sub> (70/30, v/v) at 70 °C for 4 h. **Caution:** “piranha solution” reacts violently with many organic materials and should be handled with great care. The wafers were then rinsed with distilled water and dried under a stream of nitrogen before being immersed in a 10 mM anhydrous hexane solution of OTS for 30 min at room temperature. The wafers were then rinsed with hexane and chloroform. The ellipsometric film thickness of the OTS layer was  $2.6 \pm 0.1$  nm.

**Ellipsometric Measurements.** Ellipsometric measurements were made using an automatic null ellipsometer (Rudolph Auto-EL III) equipped with a helium–neon laser (632.8 nm) that was set at an incident angle of 70°. Measurements were taken at four regions of the surface of each sample, and the mean and standard deviations were calculated. Film thicknesses were determined using the manufacturer’s program, assuming a refractive index for OTS and the LB monolayer of 1.41.

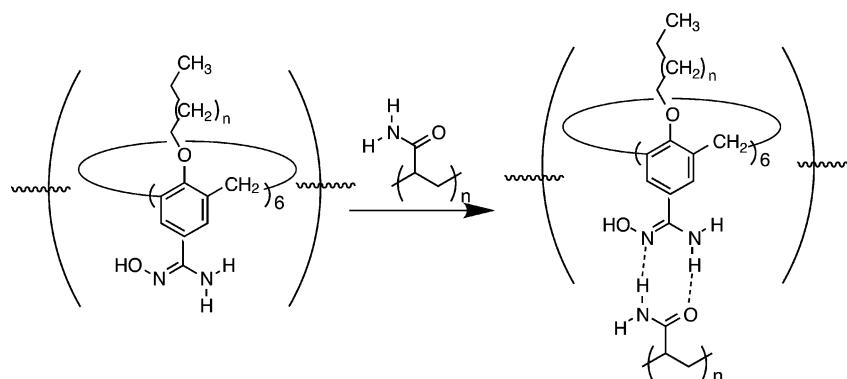
**X-ray Photoelectron Spectroscopy Measurements.** Composition and depth profiles were measured using a Scienta ESCA-300 spectrometer (Scienta Instruments AB, Uppsala, Sweden). Angle-resolved XPS measurements were performed at takeoff angles of 15 and 75°, respectively.

## Results and Discussion

To demonstrate proof of the concept, we have investigated the effects of poly(acrylamide) (PAM,  $M_w$  10 000) on (i) the cohesiveness of monolayers of 5,11,17,23,29,35-hexaamidoxime-37,38,39,40,41,42-hexakis(1-hexadecyloxy) calix[6]arene (**2**) at the air–water interface and (ii) the barrier properties of corresponding single LB bilayers (Chart 2). This specific surfactant/polymer combination was chosen on the basis of the presumption that the pendant amide units of PAM would form hydrogen bonds with the amidoxime groups of calix[6]arene (Scheme 1).<sup>10</sup> For comparison, stearoylamidoxime (SA) was also examined, because the presence of a single amidoxime group precludes the possibility of network formation with PAM.<sup>9</sup> The synthesis of

(9) Hendel, R. A.; Nomura, E.; Janout, V.; Regen, S. L. *J. Am. Chem. Soc.* **1997**, *119*, 6909–6918.

Scheme 1



calix[6]arene **2** and SA, as well as their monolayer properties, have previously been described.<sup>9</sup>

The surface pressure–area isotherm of **2** over a pure water subphase was found to be the same as that previously reported and was characterized by a limiting area of 1.60 nm<sup>2</sup>/molecule (Figure 1).<sup>9,11</sup> When PAM was added to the aqueous subphase (1 mM repeat unit concentration), **2** produced a more compressible monolayer. In this case, the limiting area increased to 1.70 nm<sup>2</sup>/molecule, and the lift-off point increased from ca. 1.90 to 2.40 nm<sup>2</sup>/mmolecule. In the absence of **2**, no surface pressure could be detected when the compressing bar of the film balance was swept over an aqueous subphase containing PAM. Taken together, these results indicate that PAM associates with the calix[6]-arene monolayer at the air–water interface.

To judge the influence that PAM has on the cohesiveness of monolayers of **2**, we measured surface viscosities using a canal viscometer in the absence and presence of PAM at 45 °C. At this temperature, the monolayer exists in the liquid-analogous state.<sup>11</sup> As is evident from the data shown in Figure 2, the monolayer that was compressed over the PAM-containing subphase showed significantly greater cohesiveness; that is, a higher surface viscosity. Similar surface viscosity measurements that were carried out with a single-chain analogue, SA, showed a precipitous drop in surface pressure in the absence and presence of PAM; that is, the surface pressure was reduced to 0 dyn/cm within 30 s at 25 °C (not shown). These results imply that the presence of multiple amidoxime headgroups of the surfactant are needed for PAM to produce a highly viscous monolayer (presumably via network formation), because **2** can have multiple associations with PAM via hydrogen bonding, but SA cannot.<sup>12,13</sup>

To determine the feasibility of incorporating PAM within LB films of **2**, a silicon wafer that had been silylated with

OTS was dipped vertically down through a monolayer of **2** (maintained at 30 dyn/cm at 25 °C over a 5 mM PAM subphase) and then pulled up, vertically, through the film into air. The transfer ratios for the down and up trips were  $0.9 \pm 0.1$  and  $1.1 \pm 0.1$ , respectively, using a dipping speed of 2 mm/min. Analysis of the resulting film by ellipsometry indicated a film thickness of  $6.2 \pm 0.23$  nm. A similar film that was prepared using a pure water subphase showed a film thickness of  $5.1 \pm 0.24$  nm. Thus, the polymer contributes ca. 1.1 nm to the overall thickness of the bilayer.<sup>14</sup> Analysis of both of these assemblies by X-ray photoelectron spectroscopy yielded further insight into their structures. Figure 3 shows the C1s spectra that were obtained using a takeoff angle of 75°. As is apparent from the amide/amidoxime carbon signal (288.0 eV), a significant amount of PAM has become incorporated into the bilayer. On the basis of the amide plus amidoxime content, relative to the amidoxime content in bilayers that were prepared in the absence of PAM, the molar ratio of PAM repeat units/amidoxime groups is estimated to be ca. 0.6. In addition, comparison of the amide and amidoxime carbon content measured using a takeoff angle of 75° with that determined using a takeoff angle of 15° indicates that both the amide and amidoxime groups are buried within the LB film. Thus, the lower takeoff angle, which measures the carbon content closer to the surface of the film, showed reduced quantities of both the amide and amidoxime groups (Table 1).

Finally, to determine whether the incorporation of PAM in LB bilayers of **2** eliminates defects, we transferred single bilayers to poly[1-(trimethylsilyl)-1-propyne] (PTMSP) support material and measured their permeability with respect to He, N<sub>2</sub>, and CO<sub>2</sub>.<sup>9</sup> In the case of He and N<sub>2</sub>, permeation across organic membranes is dominated by diffusion, where the smaller He molecule diffuses across the film at faster rates.<sup>8</sup> With CO<sub>2</sub>, solubility within the membrane also makes a significant contribution to its permeation rate.<sup>7b,8</sup> As seen in Table 2, the incorporation of PAM in bilayers of **2** resulted in a significant increase in both the He/N<sub>2</sub> and He/CO<sub>2</sub>

(10) Molecular recognition based on hydrogen bonding at the air–water interface has previously been reported: (a) Sasaki, D. Y.; Kurihara, K.; Kunitake, T. *J. Am. Chem. Soc.* **1992**, *114*, 10994–10995. (b) Kurihara, K.; Ohto, K.; Honda, Y.; Kunitake, T. *J. Am. Chem. Soc.* **1991**, *113*, 5077–5079.

(11) Hendel, R. A.; Zhang, L.-H.; Janout, V.; Conner, M. D.; Hsu, J. T.; Regen, S. L. *Langmuir* **1998**, *14*, 6545–6549.

(12) The surface viscosity of monolayers of **1**, which are not capable of forming hydrogen bonds with PAM, was found to be negligible in the absence and in the presence of this polymer. This result implies that hydrophobic interactions between the surfactant monolayer and PAM do not contribute significantly to the increased cohesiveness found with monolayers of **2**.

(13) Although the C=N stretching band of **2** (1644 cm<sup>-1</sup>) should be influenced by hydrogen bonding with PAM, the broad absorbance of the polymer (ca. 1550–1750 cm<sup>-1</sup>) precluded direct confirmation by IR spectroscopy.

(14) The ellipsometric thicknesses for single bilayers of SA, which were prepared in the absence and presence of 5 mM PAM, were  $3.3 \pm 0.1$  and  $4.2 \pm 0.1$  nm, respectively.

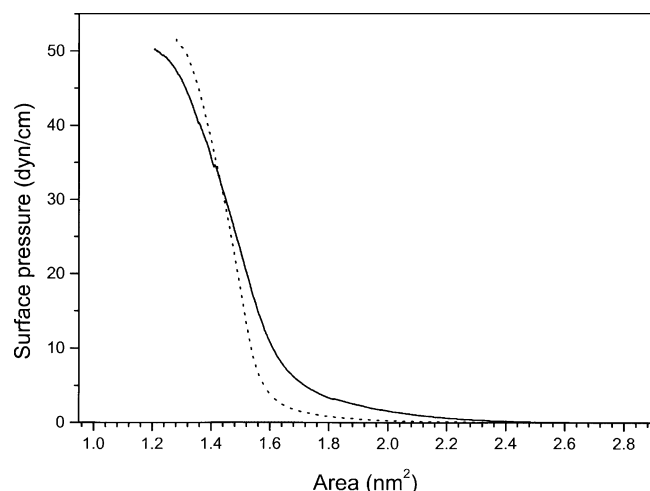


**Figure 1.** Surface pressure–area isotherm of **2** over a pure water subphase (···) and an aqueous subphase containing 5 mM PAM (—).

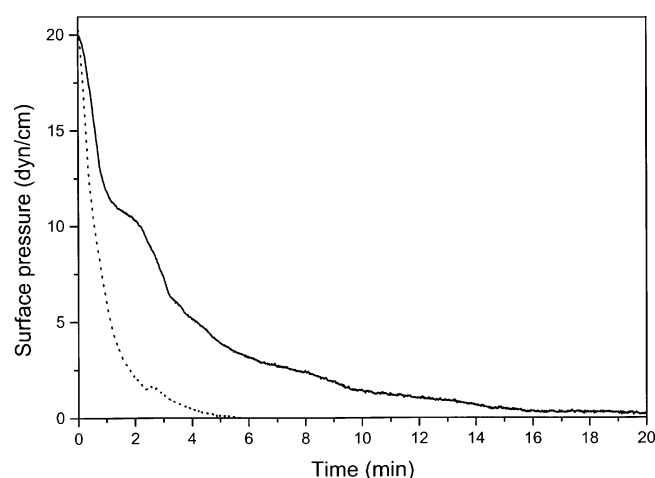


**Figure 2.** Surface pressure of monolayers of **2** over a pure (···) water subphase and an aqueous subphase containing 1 mM PAM (—) as a function of time of exposure to a 6.0 mm slit opening of a canal viscometer at 45 °C. Prior to exposure, these films were maintained for 60 min at 20 dyn/cm. During the equilibration period, the decrease in surface area was less than 5%.

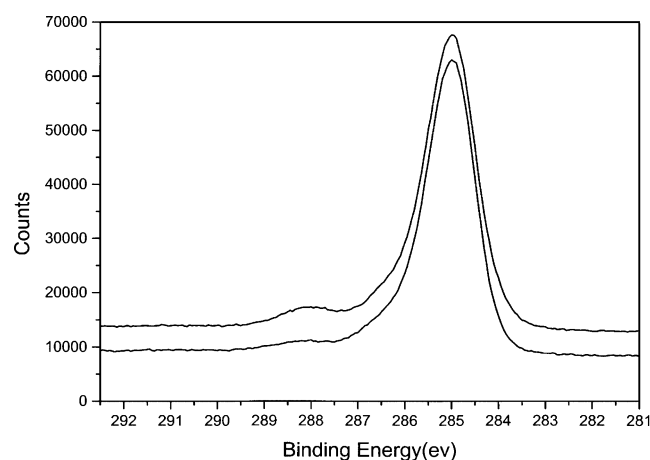


**Figure 3.** X-ray photoelectron (C1s) spectra of LB bilayers of **2** that were deposited onto silylated silicon wafers, recorded using a takeoff angle of 75°. The bilayers were fabricated using a 5 mM PAM subphase (upper curve) and a pure water subphase (lower curve), respectively.

permeation selectivities. This result clearly reflects the removal of defects within the film. In fact, on the basis of these He/N<sub>2</sub> selectivities, the quality of these PAM-glued

**Table 1. Atomic Composition of C1s in LB Bilayers**

takeoff angle (deg)	LB bilayer (surfactant)	atomic % at 288.0 eV	atomic % at 286.3 eV	atomic % at 285.0 eV
75	<b>2</b>	3.4	10.8	85.1
75	<b>2</b> /PAM	5.5	10.9	83.7
15	<b>2</b>	1.8	7.8	90.5
15	<b>2</b> /PAM	2.7	7.2	90.3

**Table 2. Normalized Flux Across LB Bilayers<sup>a</sup>**

LB bilayer	PAM <sup>b</sup>	10 <sup>6</sup> <i>P/l</i> (cm <sup>3</sup> /(cm <sup>2</sup> s cm Hg))			α <sub>He/N<sub>2</sub></sub>	α <sub>He/CO<sub>2</sub></sub>
		He	N <sub>2</sub>	CO <sub>2</sub>		
<b>2</b>		162	12.9	214	13	0.76
<b>2</b>	1.0	90	0.44	15.4	205	5.8
<b>2</b>	5.0	56	0.30	4.30	187	13.0
<b>2</b>	5.0	88	0.43	6.30	205	14.0
<b>2</b>	5.0	56	0.16	4.00	350	14.0
SA		230	245	1429	0.94	0.16
SA	5.0	231	246	1467	0.94	0.16

<sup>a</sup> LB bilayers made using a surface pressure of 30 dyn/cm (25°C). Normalized flux values (*P/l*) are the observed flux divided by the area of the membrane (9.36 cm<sup>2</sup>) and the pressure gradient (10 psi) employed; *l* is the thickness of the composite; the thickness of PTMSP in all cases was ca. 30 μm. Values reported are averages of 5–10 measurements for each sample at ambient temperatures; the error in each case was <5%. Permeation selectivities, α, are the ratio of the normalized flux values. The transfer ratios for the down and up trips were 1.0 ± 0.2 using a dipping speed of 2 mm/min. <sup>b</sup> Repeat unit concentration (mM) in the aqueous subphase.

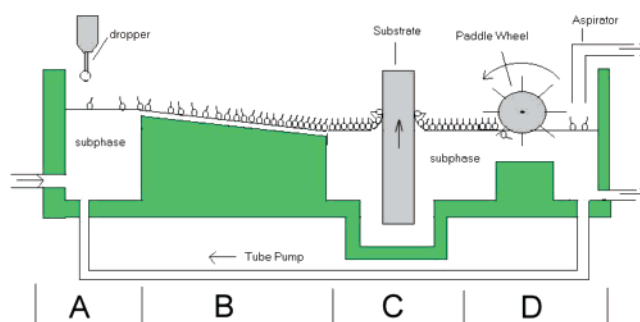


**Figure 4.** A device for forming monolayers, continuously, at the air–water interface: (A) spreading, (B) compressing, (C) depositing, and (D) aging zones.<sup>15</sup>

bilayers compares favorably with bilayers of **1** that have been glued together with PSS.<sup>7a</sup> Similar to what we have reported previously, bilayers of SA do not alter the permeability properties of PTMSP, apparently because of their disassembly and absorption into the bulk polymer (Table 2).<sup>9</sup> Thus, bilayers that were prepared from SA, using a subphase that contained 5 mM PAM, showed the identical barrier properties as that found in the absence of the polymer (Table 2).<sup>14</sup>

Recent developments in LB film technology have led to the creation of devices that allow for continuous monolayer formation at the air–water interface.<sup>15</sup> In principle, the combination of such automated LB methods (e.g., Figure 4) with large troughs (i.e., many meters in dimensions) and glued LB film materials could lead the way to the fabrication of defect-free films on a large scale. In this regard, glued LB films offer new research opportunities with an old technology that has been overshadowed in recent years by self-assembly methods.<sup>7f</sup>

(15) Albrecht, O.; Eguchi, K.; Matsuda, H.; Nakagiri, T. *Thin Solid Films* **1996**, 284–285, 152–156.

### Conclusions

The results of this study have demonstrated the feasibility of using a nonionic, water-soluble polymer (i.e., poly-(acrylamide)) that is capable of hydrogen bonding with a surfactant monolayer bearing multiple hydrogen-bonding elements (i.e., six amidoxime groups) to enhance the cohesiveness of the monolayer and allow for the construction

of defect-free LB films. This approach expands the concept of glued LB membranes, offering new possibilities for creating organized and exploitable ultrathin films.

**Acknowledgment.** This work was supported by the Department of Energy (Grant DE-FG02-05ER15720).

CM061750W